Optimization and Modelling of Cd(II) Removal from Aqueous Solution with Composite Adsorbent Prepared from *Alternanthera philoxeroides* Biochar and Bentonite by Response Surface Methodology

Yande Jing,[a,b] Xuan Wang,[a,b] Dan Wang,[a,b] and Qianqian Yang [a,b]

The current study aimed to optimize Cd(II) removal from aqueous solutions by a composite adsorbent (BCB) prepared from *Alternanthera philoxeroides* (AP) biochar (BC) and bentonite (BE) using response surface methodology (RSM). The results showed that the loading of BE did not significantly change the microstructure of BC but increased the number of functional groups. The X-ray diffraction (XRD) analysis showed that precipitation was the primary mechanism of Cd(II) adsorption. The adsorption behavior for Cd(II) fitted the Freundlich model. The pH, adsorbent dosage, and initial Cd(II) concentration were the main influencing factors affecting Cd(II) adsorption. There were significant interactions between pH and adsorbent dosage, adsorbent dosage, and initial concentration. The optimum adsorption conditions for Cd(II) with the maximum adsorption level of 89.4% were: 6.55 pH, 0.04 g adsorbent dosage, and 68.7 mg·L^{-1} initial concentration. Overall, the BCB exhibited great potential as an efficient sorbent for the Cd(II) removal from aqueous solutions.

Keywords: Biochar; Composite adsorbent; Response surface methodology; Cd(II); Bentonite

Contact information: a: College of Geography and Tourism, Qufu Normal University, 80 Yantai Road, Rizhao, Shandong, 276826, China; b: Rizhao Key Laboratory of Territory Spatial Planning and Ecological Construction, 80 Yantai Road, Rizhao, Shandong, 276826, China;
** Corresponding author: jingyande@163.com*

INTRODUCTION

Along with the rapid development of global industrialization and urbanization, a large amount of wastewater containing heavy metals is discharged into the water environment, especially in developing countries, which makes the pollution of heavy metals in water increasingly serious (Huang *et al.* 2016). Cadmium (Cd(II)), mainly from the emissions of mining and chemical enterprises, is a common heavy metal in wastewater, which can cause severe toxicity even at low concentrations (Patar *et al.* 2016). Moreover, the difficult biodegradability and easy accumulability of Cd(II) have caused a great threat to environmental safety and human health (Xu *et al.* 2016). It is imperative to search for an effective method to remove the Cd(II) from industrial wastewater. The chemical methods are commonly used methods for Cd(II) treatment, including neutralization, sulfide precipitation, adsorption, oxidation, ion exchange, electrolysis, *etc* (Purkayastha *et al.* 2014). The adsorption method has been widely used in the treatment of heavy metals in industrial wastewater due to its environmental friendliness, easy availability, and high adsorption capacity (Ma *et al.* 2016a; Zhang *et al.* 2019; Jing *et al.* 2020b).

Biochar has been found to have a well-developed pore structure and rich surface functional groups, which could remove heavy metals effectively in aqueous solution (Qian and Chen 2014; Son *et al.* 2018; Cao *et al.* 2019). *Alternanthera philoxeroides* (AP), an invasive and malignant weed in China, is an ideal raw material for biochar production (Wang *et al.* 2019; Yang *et al.* 2019). Bentonite (BE), a layered silicate mineral, has been applied to the adsorption of heavy metals gradually because of its large specific surface area and ion exchange capacity (Arbaoui and Boucherit 2014; Ren *et al.* 2014). At present, there are many studies on the application of the AP and BE as adsorbents alone in the remediation of heavy metal pollution (Huang *et al.* 2016; Ma *et al.* 2016b), but there are few studies on the combination of them into heavy metal composite adsorbents.

Traditional adsorption methods usually explore the influence of single variables such as pH value, temperature, and reaction time on adsorption efficiency (Hao *et al.* 2017). In order to determine the optimal adsorption level, the above methods are time consuming, high cost, and require a lot of manpower (Asachi and Marandi 2015). The response surface method can be used to analyze many variables that affect the adsorption effect of the experiment and establish a multiple quadratic regression equation model. Through fitting and optimizing the function relationship between multi-factor parameters and response value, the best adsorption process parameters were obtained (Biswas *et al.* 2019). It is one of the effective methods to optimize the best process parameters, reduce the number of experiments, and evaluate the level and interaction of various influencing factors method (Wang *et al.* 2017; Sharahi and Shahbazi 2017), which has been widely used in many areas of environmental pollution control and optimization experiments (Khattar and Shailza 2009; Nikraftar and Ghorbani 2017).

Composite adsorbents with different adsorption materials have shown different properties and heavy metal affinity. The authors' previous studies have shown that composite adsorbent (BCB) preparation from the biochar (BC) and the BE had good results for the removal of Cd(II) from aqueous solution (Jing *et al.* 2020a). However, the optimal adsorption parameters of the BCB for Cd(II) removal have not been determined. In this study, the BCB was used as Cd(II) adsorbent, and its physicochemical properties were characterized by Fourier-transform infrared spectroscopy (FTIR), X-ray diffraction (XRD), and scanning electron microscopy (SEM). Significant factors affecting the removal of Cd(II) were screened out by the Plackett-Burman experiment (PBE), and the optimum conditions for Cd(II) adsorption were determined by the RSM in aqueous solution.

EXPERIMENTAL

Materials

The AP was collected from a pond in Rizhao City, Shandong Province, China (35° 30' N, 119°16' E), and stored at room temperature after being air-dried, milled, and passed through a 2-mm sieve. The BE used in the experiment was purified from calcium-based BE. Its major chemical compositions were: SiO_2 67.26% (quality fraction, the same below), Al_2O_3 16.30%, Fe_2O_3 3.16%, K_2O 2.61%, CaO 4.54%, and MgO 1.57%. After simple physical purification, the calcium-based BE was screened using a 0.15-mm sieve. The Cd(II) in aqueous solution was prepared from $Cd(NO_3)_2{\cdot}4H_2O$, in which a small amount of $NaNO_3$ was added as background electrolyte. Moreover, NaOH, HCl, and HNO_3 used in the experiment were all analytically pure (Tianjin Hengxing Chemical Reagent Co., Ltd, Tianjin, China).

Adsorbents Characterization

The surface morphologies of the adsorbents were determined using SEM (JSM-5600LV; JEOL Ltd., Tokyo, Japan). Fourier-transform infrared spectroscopy (Tensor 27; Bruker, Karlsruhe, Germany) was used to analyze the surface functional groups of the adsorbents. The scanning range was 4000 cm^{-1} to 500 cm^{-1}, and the resolution was 4 cm^{-1}. The mineral components in the adsorbents were analyzed by X-ray diffraction (XRD) (D8 advance; Bruker, Karlsruhe, Germany). The tube voltage was 20 to 60 kV and the tube current was 10 to 300 mA.

The pH values of the adsorbents were determined as follows: First, 2.5 g of the adsorbent was weighed and added into 50 mL of deionized water. The adsorbent was heated in airtight conditions, boiled for 5 min, and filtered, and 5 mL of primary filtrate was discarded. The pH of the residual liquid after cooling was measured using a pH meter.

Biochar Preparation

The biochar (BC) was prepared by temperature-controlled and oxygen-limited pyrolysis conditions at 350 °C for 2 h with a heating rate of 15 °C·min^{-1}. The obtained biochar samples were ground and screened using a 100 mesh screen and labeled as BC.

The Plackett-Burman Experiment (PBE) Design

The PBE can screen out the factors that have significant influence on the adsorption effect from multiple factors. In this study, the PBE design of Cd(II) adsorption was formulated for six factors using Minitab version 18 software (Minitab LLC, State College, PA, USA), and the experimental number selected was N = 12. Variables X_1, X_2, X_3, X_4, X_5, and X_6 represented initial solution pH, initial concentration of Cd(II), dosage of composite adsorbent, adsorption temperature, adsorption time, and shaking frequency, respectively, as a single factor affecting the adsorption capacity. Two levels of low value (-1) and high value (+1) were determined for each factor, as shown in Table 1. The response value was the adsorption rate of the adsorbent for Cd(II). Concentrations of Cd(II) in the filtrate after dilution were determined by an atomic absorption spectrophotometer (GFA-7000A; Shimadzu, Kyoto, Japan) and the response value was calculated by Eq. 1,

$$R = \left(1 - \frac{C_e}{C_o}\right) \times 100\% \quad (1)$$

where R represents the response value, *i.e.*, the adsorption rate of Cd(II) (%), C_e is the concentration of Cd(II) in the solution after adsorption (mg·L^{-1}), and C_0 is the concentration of Cd(II) in the initial solution (mg·L^{-1}).

Table 1. Factors and Levels of the PBE

Investigation Factors	Levels	
	-1	+1
X_1: Solution pH	3	7
X_2: The Initial Concentration of Cd(II) (mg·L^{-1})	60	100
X_3: Dosage of Composite Adsorbent (g)	0.02	0.04
X_4: Adsorption Time (h)	2.5	5.5
X_5: Adsorption Temperature (°C)	25	40
X_6: Shaker Frequency (r·min^{-1})	110	220

The adsorption capacity of BCB, BC, and BE was calculated using Eq. 2, and the data of adsorption were fitted to both the Langmuir model (Eq. 3) and Freundlich model (Eq. 4),

$$q_e = \frac{(C_0 - C_e) \cdot V}{m} \quad (2)$$

$$q_e = \frac{q_m K C_e}{1 + K C_e} \quad (3)$$

$$q_e = K_f C_e^n \quad (4)$$

where q_e is the equilibrium adsorption capacity (mg·g^{-1}), C_0 and C_e are the initial and equilibrium concentration (mg·g^{-1}), respectively. Variable V is the volume of solution (L), m is the weight of adsorbents (g), q_m is the maximum adsorption (mg·g^{-1}), K is the adsorption equilibrium constant (L·mg^{-1}), K_f is the adsorption capacity (mg·g^{-1}), and n is the Freundlich constant.

Response Surface Optimization of Adsorption Experiment Design

The optimum conditions for Cd(II) adsorption in aqueous solutions were optimized by the multi-factor and multi-level Box-Behnken response surface optimization method. Contour maps and three-dimensional stereograms were established to test the adaptability and significance of the model, thereby optimizing the adsorption parameters of composite adsorbent for Cd(II). The second-order model formula of the RSM was derived from the Numerical Solution function of Design-Expert 8.0 software (Stat-Ease, Inc., Minneapolis, MN, USA) as follows,

$$y = \beta_0 + \sum_{i=0}^{h} \beta_i \chi_i + \sum_{i<1}^{h} \beta_{ij} \chi_i \chi_j + \sum_{i=1}^{h} \beta_{ii} \chi_i^2 \quad (5)$$

where y is the predicted response variable (%), β_0, β_i, and β_{ij} are the constant regression coefficients of the model, and χ_i and χ_j are the independent variables in the form of coded values.

RESULTS AND DISCUSSION

Physicochemical Properties of Absorbents

The FTIR spectra of the BCB, BC, and BE are shown in Fig. 1. The recognition of the obtained spectra had a typical peak of -OH group at 3615 to 3423 cm^{-1} (Yu *et al.* 2018). The absorption peak near the 2990 to 2835 cm^{-1} was an aliphatic -CH_2 stretching vibration peak. However, there was no similar absorption peak in the BE spectrum, indicating no aliphatic group in the BE. The peak at 1625 cm^{-1} represented the stretching vibrations of C=O and C=C, corresponding to aromatic characteristics. Compared with BE, BCB, and BC had more obvious vibration peaks, indicated that the BCB and BC had more carbonyl functional groups and complex aromatic structures. The stretching vibration peak near 1395 to 1303 cm^{-1} represented the C-O. The sharp vibrational peak at 1039 cm^{-1} in the BCB and BE was caused by structural vibration of Si-O tetrahedron and Al-O octahedron of the BE (Liu *et al.* 2011), which was an important feature of the BE particle loaded on the surface of biochar. The stretching vibration peak near band 753 cm^{-1} was considered to the vibration of inorganic functional group Si-O-Si (Qian and Chen 2013). In this study, the number of functional groups of the BCB, BC, and BE might significantly affect the adsorption capacity of Cd(II).

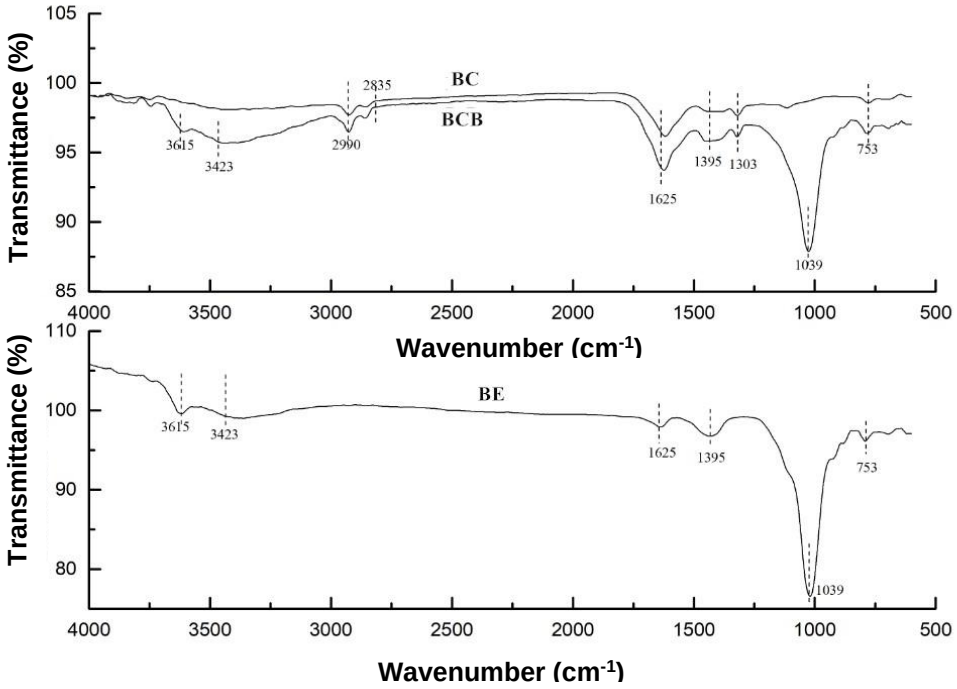

Fig. 1. FTIR spectra of BC, BCB, and BE

SEM images of BCB, BC, and BE at different magnification (500 times (a, d, g), 1000 times (b, e, h), and 2000 times (c, f, i), from left to right) are shown in Fig. 2.

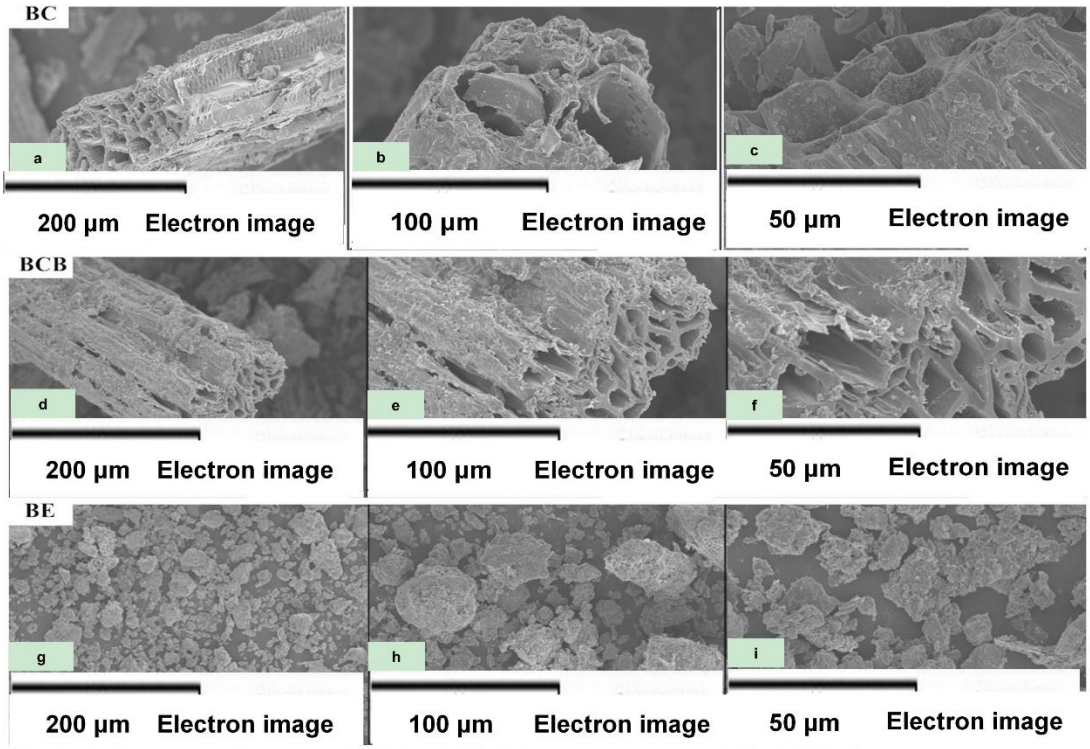

Fig. 2. SEM images of the BC (a, b, c), BCB (d, e, f), and BE (g, h, i) before and after Cd(II) adsorption by the BCB

From the micrographs, the samples of BC and BCB had typical microscopic morphology of plant-derived biochar: intact tubular structure and distinct pore structure (Keiluweit *et al.* 2010; Lian and Xing 2017). These better microporous and developed pore structures (with more holes and larger aperture) facilitated the binding of Cd(II) with more adsorption sites. The BC had a thickly layered structure and smooth external morphology, while the surface of the BCB was covered with a layer of layered sediments similar to the morphology of the BE, indicating that BE particles were loaded on the surface of biochar successfully. Compared with the BC, there was no significant change in SEM images of the BCB, which was attributed to the fact that the BE particles were mainly loaded on biochar by physical methods during the preparation of BCB. The SEM images of the BE were different from the BC and BCB, and its morphologies were agglomerated structure with large voids. This might be the result of the active surface polarity and surface energy of the BE, which was conducive to the preparation of composite adsorbents (Bilgic *et al.* 2014) with high adsorption performance by modification or compounding with organic/inorganic materials.

The XRD spectrum of BCB before (a) and after (b) Cd(II) adsorption is shown in Fig. 3. The relatively broad amorphous diffraction peaks did not appear in the range of 10° to 50°, most of which were sharp crystal diffraction peaks. For example, the 2θ = 26.5° might be the characteristic diffraction peak of graphite crystal. It could be inferred that higher polymeric aromatic rings might contain in the carbon molecular structure (Popova 2018). In the spectrum of BCB + Cd, the sharp diffraction peaks' intensity between 2θ = 20° to 22° decreased, which might be caused by the separation of the BE particles loaded on the surface of biochar from biochar or the oxidation of oxygen-containing functional groups during the vibration process (Fan *et al.* 2010). Additionally, the new diffraction peaks (α) emerged, indicating that the new precipitated materials were formed after Cd(II) adsorption and the primary mechanism of Cd(II) adsorption by the BCB was surface precipitation (Zhou *et al.* 2013).

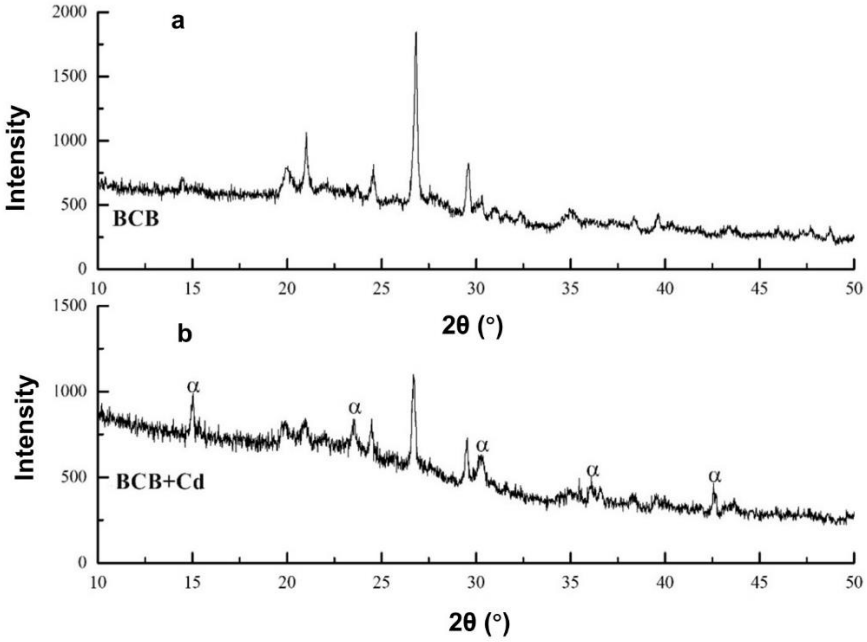

Fig. 3. XRD spectrum before (a) and after (b) Cd(II) adsorption by the BCB

Plackett-Burman Experiment Analysis

The response values of the PBE design are shown in Table 2, and the variance analysis results of the regression model (ANOVA) showed that the P-value of the model was 0.0054 ($P < 0.05$), indicating that the model was statistically significant within the selected level range (Deng *et al.* 2017). According to the P-values of the six factors, the factors affecting adsorption rate were $X_1 > X_2 > X_3 > X_5 > X_4 > X_6$ in order of influence. The significant factors ($P < 0.05$): X_1, X_2, and X_3, *i.e.*, the pH, the initial concentration, and the adsorbent dosage, were assessed as crucial factors in the steepest climbing and response surface optimization analysis experiments. Factors X_4, X_5, and X_6 ($P > 0.05$) had no significant difference. However, that did not mean that they did not affect the Cd(II) adsorption in the solution. The data of the model coefficient effect showed that factor X_1 and X_3 were positively correlated with the response value and negatively correlated with the X_2.

The determination coefficient $R^2 = 0.9861$ indicated that the model had high significance, accuracy, and reliability. In addition, the adjusted determination coefficient $R^2_{adj} = 0.9693$ indicated that the model can explain 96.93% of variability of the experimental data.

Table 2. The Results of the PBE Design

Run	X_1	X_2	X_3	X_4	X_5	X_6	Adsorption
	pH	Concen-tration	Dosage	Time	Temper-ature	Shaker Frequency	%
		$mg \cdot L^{-1}$	g	h	℃	$r \cdot min^{-1}$	
1	1	-1	-1	-1	1	1	89.26
2	1	-1	1	-1	-1	-1	94.33
3	1	1	-1	1	1	-1	77.87
4	1	-1	1	1	-1	1	93.32
5	1	1	1	-1	1	1	90.63
6	1	1	-1	1	-1	-1	73.00
7	-1	1	1	-1	1	-1	36.50
8	-1	1	-1	-1	-1	1	29.51
9	-1	-1	-1	1	1	1	51.21
10	-1	1	1	1	-1	1	40.25
11	-1	-1	1	1	1	-1	60.65
12	-1	-1	-1	-1	-1	-1	46.16

Significant Single Factor Steepest Climbing Design

Based on the influence of each factor, the steepest climbing experiment design was adopted to approach the optimal value region efficiently. The significant factors were selected from the PBE analysis of variance, and the gradient size and climbing direction could be determined by the effective value of significant factors in the PBE. The design of the steepest climbing experiment was formulated according to the following steepest ascent gradients of a key single factor: the critical single factor pH (3, 4, 5, 6, and 7), the initial concentration of cadmium (20, 40, 70, 90, and 120 $mg \cdot L^{-1}$), and the dosage of composite adsorbent (0.01, 0.02, 0.03, 0.04, and 0.05 g).

Effect of the pH, Initial Concentration, and Adsorbent Dosage

As shown in Fig. 4, the adsorption rate (R) and adsorption capacity (q_e) increased continuously with the pH from 3 to 5, with the growth rate, reaching 45.0% and 42.2%,

respectively. The R and q_e tended to be smoothly saturated in the range of pH 5 to 7 because of the weak competition of cations, the strong precipitation of anions (OH^-, CO_3^{2-}, PO_4^{3-}, *etc*.), and Cd(II) in solution (Huang *et al.* 2011; Hubbe *et al.* 2011). In addition, the low pH condition meant the high concentration of H^+ in solution, the functional groups (hydroxyl, carboxyl, carbonyl, *etc*.) of the adsorbent were prone to H^+ binding. Moreover, electrostatic repulsion and competitive adsorption between the cations (Ca^{2+}, K^+, and Mg^{2+}) and Cd(II) weakened the adsorption performance of adsorbents due to the dissolution of mineral crystal components (Wang *et al.* 2015). Therefore, higher solution pH was favorable for Cd(II) adsorption, and the order of the R and q_e was BCB > BC > BE under the pH < 5.5, indicating that the composite adsorbent had a higher adsorption effect under acidic conditions.

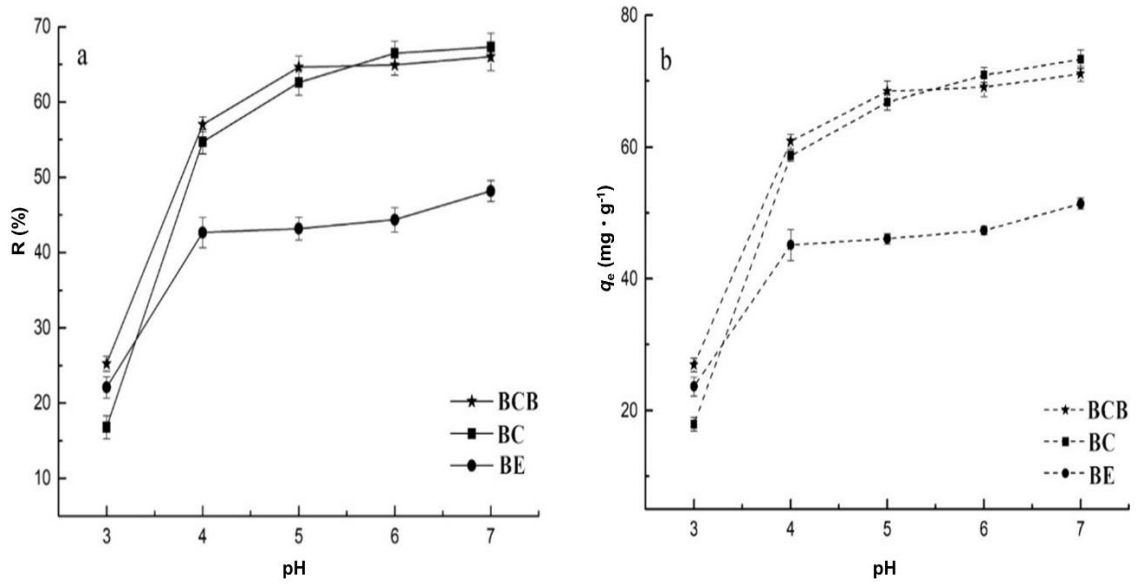

Fig. 4. Effect of pH on Cd(II) adsorption under temperature 25 °C, initial concentration 80 mg·L^{-1}, contact time 24 h, dose 0.03 g: (a) the adsorption rate of Cd(II) and (b) the adsorption capacity of Cd(II)

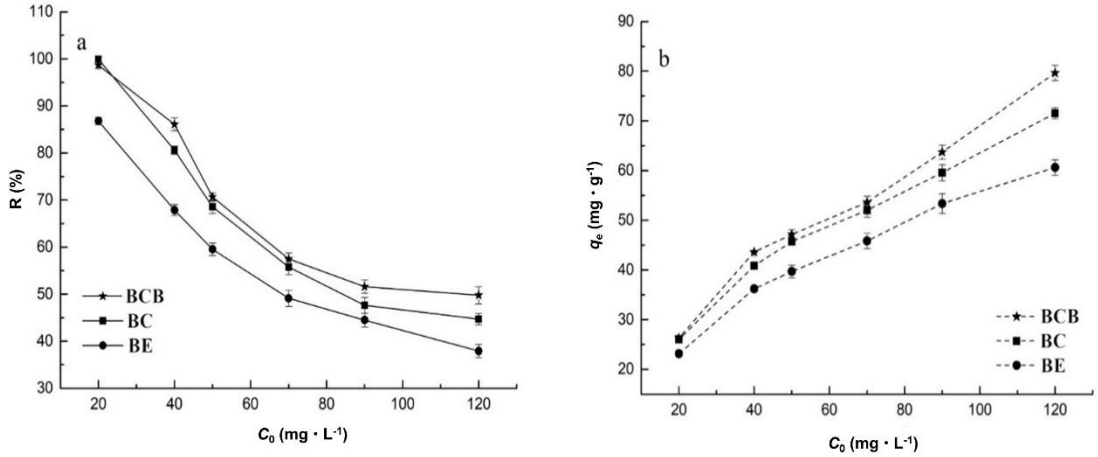

Fig. 5. Effect of initial concentration on Cd(II) adsorption under temperature 25 °C, contact time 24 h, dose 0.03 g, and pH at 4: (a) the adsorption rate of Cd(II) and (b) the adsorption capacity of Cd(II)

Figure 5 indicates the changing trend of the R and q_e of Cd(II) adsorbed by the BCB, BC, and BE with the Cd(II) initial concentration. The results showed that the q_e increased with the increase of the Cd(II) initial concentration, while the adsorption rate was the opposite. The adsorbent could provide sufficient adsorption sites at a lower Cd(II) initial concentration. However, the active adsorption sites decreased gradually as the Cd(II) initial concentration increased, and the adsorption process changed into pore adsorption, resulting in a decrease of adsorption rate (Liu *et al.* 2010).

The fitting parameters of Langmuir and Freundlich models are listed in Table 3. The better appropriate prediction for Cd(II) adsorption was provided by the Freundlich model, as it had a higher coefficient of determination (R^2) than the Langmuir model., and the adsorption capacity would rise continuously with the increase of the initial concentration of Cd(II) (Wang *et al.* 2018). It was noted that R^2 of the Langmuir model was also very high. Since Cd(II) adsorption involved specific adsorption and non-specific adsorption, and was affected by physicochemical properties of the composite adsorbent, it was also very complex to describe the law from limited data by mathematical methods. Therefore, the hypothesis of the Freundlich model did not negate the hypothesis of Langmuir model.

Table 3. Langmuir and Freundlich Fitting Results on Cd(II) Adsorption

Sample	Temperature (K)	Langmuir			Freundlich		
		K ($mg \cdot L^{-1}$)	q_m ($mg \cdot g^{-1}$)	R^2	K_f	n	R^2
BCB	298	0.0234	123.68	0.9798	5.64	0.5664	0.9907
	313	0.0108	138.31	0.9849	5.89	0.5955	0.9937
BC	298	0.0156	100.99	0.9775	5.31	0.5169	0.9933
	313	0.0147	107.61	0.9803	5.67	0.5306	0.9919
BE	298	0.0193	78.11	0.9873	5.02	0.4724	0.9916
	313	0.0162	90.11	0.9896	5.35	0.5102	0.9934

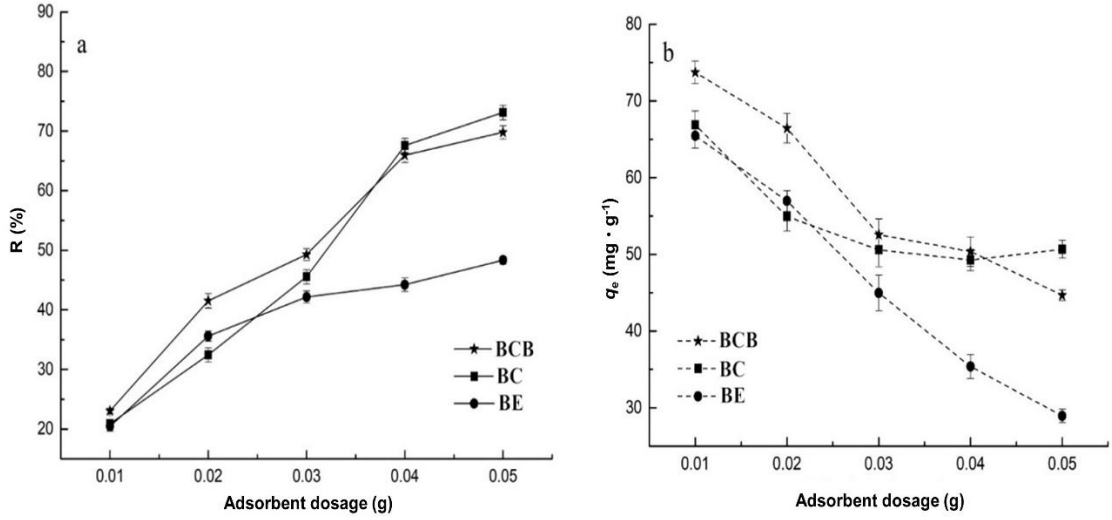

Fig. 6. Effect of the adsorbent dosage on Cd(II) adsorption under temperature 25 °C, initial concentration 80 $mg \cdot L^{-1}$, contact time 24 h, and pH at 4: (a) the adsorption rate of Cd(II) and (b) the adsorption capacity of Cd(II)

The influence of the adsorbent dosage on Cd(II) adsorption was evaluated. It could be seen from Fig. 6 that the R values of BCB and BC increased from 20.0% to more than 70% when the absorbent dose was increased from 0.01 to 0.05 g. On the contrary, the q_e decreased significantly, which might be that the active surface area of the adsorbent decreased with continued increment in the adsorbent dosage within a certain volume (Wang *et al.* 2010). More active adsorption sites and functional groups could be provided when the adsorbent dosage increased, which promoted the adsorption effect. Furthermore, the adsorption effect of BCB was the best when the dosage was less than 0.04 g, which might be related to the change in the adsorption properties of the BE.

Optimization of Cd(II) Adsorption by Composite Adsorbents

Based on the results of the PBE and the steepest climbing experiment, it was determined that the pH, the initial concentration, and the adsorbent dosage were the main factors affecting the adsorption effect of Cd(II). Therefore, the design of the Box-Behnken response surface optimization experiment was made based on the following codes and levels of independent variables: the pH (3 (code, -1), 5 (code, 0), 7 (code, +1)), the initial concentration of cadmium (60 mg·L^{-1} (code, -1), 80 mg·L^{-1} (code, 0), 100 mg·L^{-1} (code, +1)), and the dosage of composite adsorbent (0.02 g (code, -1), 0.03 g (code, 0), and 0.04 g (code, +1)).

The Box-Behnken design matrix consisted of 17 trials, as shown in Table 4. The second-order polynomial equation (Y_m) was established by response surface regression analysis based on Eq. 2:

$$Y_m = 75.46 + 14.74A + 8.67B - 3.96C - 0.14AC + 4.34AB + 2.69BC - 12.36A^2 - 2.48B^2 - 1.22C^2 \quad (6)$$

Table 4. The Results of Box-Behnken Design Matrix in Coded

Run	*A*	*B*	*C*	Adsorption Rate (%)
	pH	Dosage (g)	Concentration (mg·L^{-1})	
1	-1	0	1	41.94
2	0	-1	1	55.19
3	1	1	0	85.72
4	0	1	-1	82.96
5	0	0	0	75.01
6	-1	0	-1	49.69
7	0	0	0	75.56
8	-1	-1	0	44.21
9	1	0	-1	82.12
10	0	0	0	75.72
11	-1	1	0	50.22
12	0	0	0	75.86
13	0	0	0	75.62
14	0	1	1	80.54
15	1	-1	0	62.33
16	0	-1	-1	68.37
17	1	0	1	73.79

The ANOVA results of response values showed that the regression model had a $P < 0.0001$ and the "lack of fit P-value" of 0.36, *i.e.*, the model was very significant. Number 65.21 of the given F-value and 0.99 of the R^2 value revealed that the model was suitable for describing the relationship between each independent variable, *i.e.*, pH (*A*), Cd(II) initial concentration (*B*), dosage (*C*), and response value. In conclusion, the response surface model was suitable for optimizing the adsorption of CD(II) adsorption on the composite adsorbents.

Because the P-values of all coefficients were $P < 0.05$, expect *AC* and C^2, it meant that these were significant or very significant, including linear effects (*A*, *B*, and *C*), interactive effects (*AB* and *BC*) and quadratic terms (A^2 and B^2). Thus, the influences of three key factors on the response value were not only the linear effect but also the interactive and quadratic effect.

In order to intuitively express the influences of various factors on the response value, the response surface contours are shown in Figs. 7a to 7f.

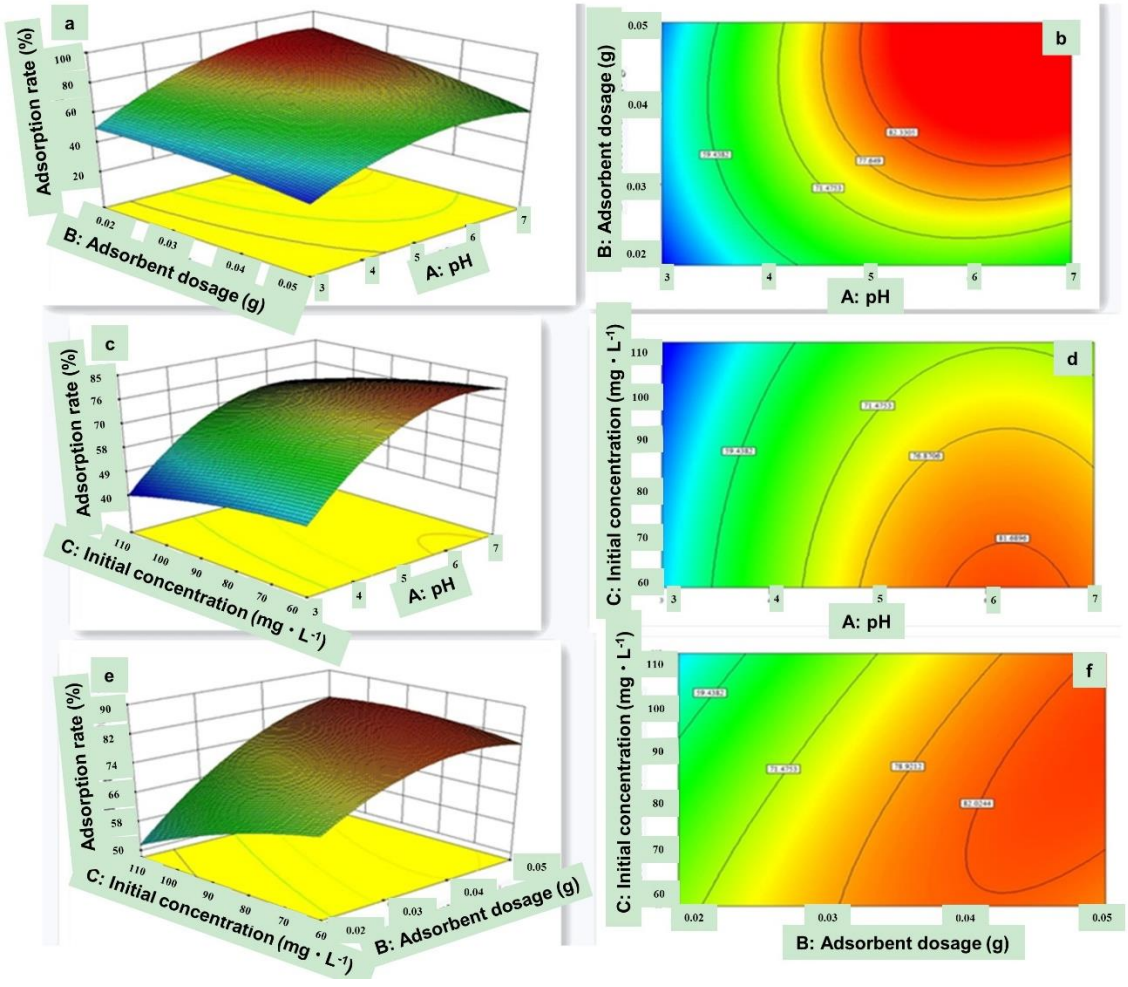

Fig. 7. Variation of response surface (a, c, and e) and contour plots of adsorption rate of interaction (b) between pH and adsorbent dosage, interaction (d) between pH and initial concentration, and interaction (f) between adsorbent dosage and initial concentration

The significant interaction terms: AB (the pH and the adsorbent dosage) and BC (the adsorbent dosage and the initial concentration) were determined by the P-value from ANOVA in the previous section. The response surface contours (Fig. 7a) were convex with an open downward direction, indicating that the interaction of *AB* had a significant effect on the adsorption rate. When the initial concentration was the center value (80 $mg \cdot L^{-1}$), the higher pH accompanied by the higher adsorbent dosage enhanced the response value, which was consistent with the results of the single-factor steepest climbing experiment. The contour plot (Fig. 7b) showed that the increase of pH had a more obvious effect on the Cd(II) adsorption than the adsorbent dosage (Fathianpour *et al.* 2018).

When the adsorbent dosage was the center value (0.03 g), the effect of interaction term *AC* (the pH *versus* the initial concentration) on the response value (Fig. 7c) showed the reverse effect of the initial concentration and the positive effect of the pH on the Cd(II) adsorption. Similar to the results of the single-factor experiment, the higher pH accompanied by the lower initial concentration also slightly enhanced the Cd(II) adsorption, although the ANOVA was not significant ($P = 0.8901$). The contour plot (Fig. 7d) showed that the maximum response value was at the lower right corner, including 0.04 g of the adsorbent dosage and the pH of 7. Moreover, the pH was more effective than the initial concentration according to the contour line directions (Fig. 7d).

Figures 7e and 7f illustrate the interaction term of *BC* (the adsorbent dosage *versus* the initial concentration) on response value when the pH was at 7 of the central value. The results showed that increasing the adsorbent dosage at low initial concentration could significantly improve the adsorption effect of Cd(II), and the response surface (Fig. 7e) was steep, indicating that the initial concentration and the adsorbent dosage had a significant impact on the Cd(II) adsorption. In addition, the elliptical contour plot (Fig. 7f) represented that the interaction term of *BC* was significant (Omar and Amin 2011), which was consistent with the ANOVA in the previous section ($P = 0.0325$). Therefore, the maximum response value was obtained at 0.04 g of the adsorbent dosage and 60 $mg \cdot L^{-1}$ of the initial concentration.

Adsorption Parameters Optimization and Verification Test

The optimal adsorption combination given by the second-order model formula of the RSM could adsorb 89.4% Cd(II) from 40 mL solution under the condition of pH 6.55, the adsorbent dosage of 0.04 g, and the initial concentration of 68.7 $mg \cdot L^{-1}$. The verification test was carried out under the above optimal conditions (three groups of parallel tests), and the results showed that the adsorption rates for Cd(II) were 91.3%, 91.9%, and 86.5% in the three groups of parallel tests, respectively, which were close to the predicted values.

CONCLUSIONS

1. As an efficient sorbent, the composite adsorbent with biochar and bentonite (BCB) exhibited great potential for Cd(II) removal from aqueous solutions. The adsorption data of adsorbents was well fitted by the Langmuir and Freundlich models.
2. The crucial factors affecting Cd(II) adsorption were the pH, the initial concentration, and the adsorbent dosage through the Plackett-Burman experimental design (PBE), which were further optimized by response surface methodology (RSM). The optimum adsorption conditions for Cd(II) with the maximum adsorption rate of 89.4% were: 6.55

pH, 0.04 g adsorbent dosage, and 68.7 $mg \cdot L^{-1}$ initial Cd(II) concentration.

3. The combination of PBE and RSM could effectively screen out the main influencing factors and optimize the best process parameters.

ACKNOWLEDGMENTS

This research was supported by the Natural Science Foundation of Shandong Province (No. ZR2013DM005). The authors extend sincere gratitude to Xuan Wang for help setting up and running the experiments.

REFERENCES CITED

Arbaoui, F., and Boucherit, M. N. (2014). "Comparison of two Algerian bentonites: Physico-chemical and retention capacity study," *Appl. Clay Sci.* 91-92, 6-11. DOI: 10.1016/j.clay.2014.02.001

Asachi, M., and Marandi, R. (2015). "Response surface modeling of lead and copper removal from oil field brine by potential sorption method," *Part. Sci. Technol.* 33(3), 290-300. DOI: 10.1080/02726351.2014.908255

Bilgic, C., Yazici, D. T., Karakehya, N., Cetinkaya, H., Singh, A., and Chehimi, M. M. (2014). "Surface and interface physicochemical aspects of intercalated organo-bentonite," *Int. J. Adhes. Adhes.* 50, 204-210. DOI: 10.1016/j.ijadhadh.2014.01.033

Biswas, S., Bal, M., Behera, S. K., Sen, T. K., and Meikap, B. C. (2019). "Process optimization study of Zn^{2+} adsorption on biochar-alginate composite adsorbent by response surface methodology (RSM)," *Water* 11(2), Article number 325. DOI: 10.3390/w11020325

Cao, Y., Jing, Y., Hao, H., and Wang, X. (2019). "Changes in the physicochemical characteristics of peanut straw biochar after freeze-thaw and dry-wet aging treatments of the biomass," *BioResources* 14(2), 4329-4343. DOI: 10.15376/biores.14.2.4329-4343

Deng, X., Zhou, H., Qu, X. N., Long, J., Peng, P. Q., Hou, H. B., Li, K. L., Zhang, P., and Liao, B. H. (2017). "Optimization of Cd(II) removal from aqueous solution with modified corn straw biochar using Plackett-Burman design and response surface methodology," *Desalin. Water Treat.* 70, 210-219. DOI: 10.5004/dwt.2017.20499

Fan, Z. J., Wang, K., Wei, T., Yan, J., Song, L. P., and Shao, B. (2010). "An environmentally friendly and efficient route for the reduction of graphene oxide by aluminum powder," *Carbon* 48(5), 1686-1689. DOI: 10.1016/j.carbon.2009.12.063

Fathianpour, A., Taheriyoun, M., and Soleimani, M. (2018). "Lead and zinc stabilization of soil using sewage sludge biochar: Optimization through response surface methodology," *Clean-Soil Air Water* 46(5), Article ID 1700429. DOI: 10.1002/clen.201700429

Hao, H., Jing, Y. D., Ju, W. L., Shen, L., and Cao, Y. Q. (2017). "Different types of biochar: Effect of aging on the Cu(II) adsorption behavior," *Desalin. Water Treat.* 95, 227-233. DOI: 10.5004/dwt.2017.21524

Huang, X. X., Liu, Y. G., Liu, S. B., Li, Z. W., Tan, X. F., Ding, Y., Zeng, G. M., Xu, Y., Zeng, W., and Zheng, B. H. (2016). "Removal of metformin hydrochloride by

Alternanthera philoxeroides biomass derived porous carbon materials treated with hydrogen peroxide," *RSC Advances* 6(83), 79275-79284. DOI: 10.1039/c6ra08365j

Huang, Y. H., Shih, Y. J., and Chang, C. C. (2011). "Adsorption of fluoride by waste iron oxide: The effects of solution pH, major coexisting anions, and adsorbent calcination temperature," *J. Hazard. Mater.* 186(2-3), 1355-1359. DOI: 10.1016/j.jhazmat.2010.12.025

Hubbe, M. A., Hasan, S. H., and Ducoste, J. J. (2011). "Cellulosic substrates for removal of pollutants from aqueous systems: A review. 1. Metals," *BioResources* 6(2), 1-201. DOI: 10.5552/drind.2011.1106

Jing, Y. D., Cao, Y. Q., Yang, Q. Q., and Wang, X. (2020a). "Removal of Cd (II) from aqueous solution by clay-biochar composite prepared from *Alternanthera philoxeroides* and bentonite," *BioResources* 15(1), 598-615. DOI: 10.15376/biores.15.1.598-615

Jing, Y. D., Shen, L., and Cao, Y. Q. (2020b). "Animal or plant waste-derived biochar for Cd(II) immobilization: Effects of freeze-thaw-wet-dry cyclic aging on adsorption behavior in tea garden soils," *Desalin. Water Treat.* 182, 187-193. DOI: 10.5004/dwt.2020.25192

Keiluweit, M., Nico, P. S., Johnson, M. G., and Kleber, M. (2010). "Dynamic molecular structure of plant biomass-derived black carbon (biochar)," *Environ. Sci. Technol.* 44(4), 1247-1253. DOI: 10.1021/es9031419

Khattar, J. I. S., and Shailza, L. (2009). "Optimization of Cd^{2+} removal by the cyanobacterium *Synechocystis pevalekii* using the response surface methodology," *Process Biochem.* 44(1), 118-121. DOI: 10.1016/j.procbio.2008.09.015

Lian, F., and Xing, B. S. (2017). "Black carbon (biochar) in water/soil environments: Molecular structure, sorption, stability, and potential risk," *Environ. Sci. Technol.* 51(23), 13517-13532. DOI: 10.1021/acs.est.7b02528

Liu, Q. S., Zheng, T., Wang, P., Jiang, J. P., and Li, N. (2010). "Adsorption isotherm, kinetic and mechanism studies of some substituted phenols on activated carbon fibers," *Chem. Eng. J.* 157(2-3), 348-356. DOI: 10.1016/j.cej.2009.11.013

Liu, Z. R., Uddin, M. A., and Sun, Z. X. (2011). "FT-IR and XRD analysis of natural Na-bentonite and Cu(II)-loaded Na-bentonite," *Spectrochim. Acta, Part A* 79(5), 1013-1016. DOI: 10.1016/j.saa.2011.04.013

Ma, L. Y., Chen, Q. Z., Zhu, J. X., Xi, Y. F., He, H. P., Zhu, R. L., Tao, Q., and Ayoko, G. A. (2016a). "Adsorption of phenol and Cu(II) onto cationic and zwitterionic surfactant modified montmorillonite in single and binary systems," *Chem. Eng. J.* 283, 880-888. DOI: 10.1016/j.cej.2015.08.009

Ma, J., Su, G. J., Zhang, X. P., and Huang, W. (2016b). "Adsorption of heavy metal ions from aqueous solutions by bentonite nanocomposites," *Water Environ. Res.* 88(8), 741-746. DOI: 10.2175/106143016x14609975747081

Nikraftar, N., and Ghorbani, F. (2017). "Synthesis of magnetic nanohybrid of Fe3+-TMSPT-MNPs as a novel adsorbent: Optimization of Cr(VI) adsorption by response surface methodology," *Desalin. Water Treat.* 76, 241-253. DOI: 10.5004/dwt.2017.20625

Omar, W. N. N. W., and Amin, N. A. S. (2011). "Optimization of heterogeneous biodiesel production from waste cooking palm oil *via* response surface methodology," *Biomass Bioenerg.* 35(3), 1329-1338. DOI: 10.1016/j.biombioe.2010.12.049

Patar, A., Giri, A., Boro, F., Bhuyan, K., Singha, U., and Giri, S. (2016). "Cadmium pollution and amphibians - Studies in tadpoles of *Rana limnocharis*," *Chemosphere* 144, 1043-1049. DOI: 10.1016/j.chemosphere.2015.09.088

Popova, A. N. (2018). "Crystallographic analysis of graphite by X-Ray diffraction," *Coke Chem.* 60(9), 361-365. DOI: 10.3103/s1068364x17090058

Purkayastha, D., Mishra U., and Biswas S. (2014). "A comprehensive review on Cd(II) removal from aqueous solution, " *J. Water Process Eng.* 2, 105-128. DOI:10.1016/j.jwpe.2014.05.009

Qian, L. B., and Chen, B. L. (2013). "Dual role of biochars as adsorbents for aluminum: The effects of oxygen-containing organic components and the scattering of silicate particles," *Environ. Sci. Technol.* 47(15), 8759-8768. DOI: 10.1021/es401756h

Qian, L. B., and Chen, B. L. (2014). "Interactions of aluminum with biochars and oxidized biochars: Implications for the biochar aging process," *J. Agric. Food Chem.* 62(2), 373-380. DOI: 10.1021/jf404624h

Ren, W., Teng, Y., Zhou, Q., Paschke, A., and Schuurmann, G. (2014). "Sorption of chlorimuron-ethyl on montmorillonite clays: Effects of exchangeable cations, pH, and ionic strength," *Environ. Sci. Pollut. Res. Int.* 21(19), 11587-11597. DOI: 10.1007/s11356-014-3139-6

Sharahi, F. J., and Shahbazi, A. (2017). "Melamine-based dendrimer amine-modified magnetic nanoparticles as an efficient Pb(II) adsorbent for wastewater treatment: Adsorption optimization by response surface methodology," *Chemosphere* 189, 291-300. DOI: 10.1016/j.chemosphere.2017.09.050

Son, E. B., Poo, K. M., Chang, J. S., and Chae, K. J. (2018). "Heavy metal removal from aqueous solutions using engineered magnetic biochars derived from waste marine macro-algal biomass," *Sci. Total Environ.* 615, 161-168. DOI: 10.1016/j.scitotenv.2017.09.171

Wang, F. Y., Wang, H., and Ma, J. W. (2010). "Adsorption of cadmium (II) ions from aqueous solution by a new low-cost adsorbent-Bamboo charcoal," *J. Hazard. Mater.* 177(1-3), 300-306. DOI: 10.1016/j.jhazmat.2009.12.032

Wang, G. Y., Zhang, S. R., Yao, P., Chen, Y., Xu, X. X., Li, T., and Gong, G. S. (2018). "Removal of Pb(II) from aqueous solutions by *Phytolacca americana* L. biomass as a low cost biosorbent," *Arabian J. Chem.* 11(1), 99-110. DOI: 10.1016/j.arabjc.2015.06.011

Wang, H. Y., Gao, B., Wang, S. S., Fang, J., Xue, Y. W., and Yang, K. (2015). "Removal of Pb(II), Cu(II), and Cd(II) from aqueous solutions by biochar derived from KMnO4 treated hickory wood," *Bioresource Technol.* 197, 356-362. DOI: 10.1016/j.biortech.2015.08.132

Wang, X., Jing, Y. D., Cao, Y. Q., Xu, S., and Chen, L. D. (2019). "Effect of chemical aging of *Alternanthera philoxeroides*-derived biochar on the adsorption of Pb (II)," *Water Sci. Technol.* 80(2), 329-338. DOI: 10.2166/wst.2019.276

Wang, Y. H., Lv, W. Y., Zou, X. G., Shou, R. J., Huang, J. L., Yao, K., and Liu, G. G. (2017). "The study of adsorption mechanism of Cu(II) from aqueous solutions by humin with response surface methodology," *Acta Sci. Circumstantiae* 37(2), 624-632. DOI: 10.13671/j.hjkxxb.2016.0268

Xu, P., Sun, C. X., Ye, X. Z., Xiao, W. D., Zhang, Q., and Wang, Q. (2016). "The effect of biochar and crop straws on heavy metal bioavailability and plant accumulation in a Cd and Pb polluted soil," *Ecotoxicol. Environ. Saf.* 132, 94-100. DOI: 10.1016/j.ecoenv.2016.05.031

Yang, Y., Wei, Z. B., Zhang, X. L., Chen, X., Yue, D. M., Yin, Q., Xiao, L., and Yang, L. Y. (2014) . "Biochar from *Alternanthera philoxeroides* could remove Pb(II) efficiently," *Bioresour. Technol.* 171, 227-232. DOI:10.1016/j.biortech.2014.08.015

Yu, J. G., Zhang, X. W., Wang, D., and Li, P. (2018). "Adsorption of methyl orange dye onto biochar adsorbent prepared from chicken manure," *Water Sci. Technol.* 77(5), 1303-1312. DOI: 10.2166/wst.2018.003

Zhang, L. X., Tang, S. Y., He, F. X., Liu, Y., Mao, W., and Guan, Y. T. (2019). "Highly efficient and selective capture of heavy metals by poly(acrylic acid) grafted chitosan and biochar composite for wastewater treatment," *Chem. Eng. J.* 378, DOI: 10.1016/j.cej.2019.122215

Zhou, Y. M., Gao, B., Zimmerman, A. R., Fang, J., Sun, Y. N., and Cao, X. D. (2013). "Sorption of heavy metals on chitosan-modified biochars and its biological effects," *Chem. Eng. J.* 231, 512-518. DOI: 10.1016/j.cej.2013.07.036

Article submitted: June 24, 2020; Peer review completed: August 23, 2020; Revised version received and accepted: October 7, 2020; Published: October 26, 2020.
DOI: 10.15376/biores.15.4.9413-9428